American Mineralogist, Volume 59, pages 143–151, 1974

Mössbauer Studies of Natural Biotites

HANS ANNERSTEN[1]

Institute of Geology, Division of Mineralogy and Petrology, University of Uppsala, Sweden

Abstract

Natural biotites with atomic ratios (Fe/Fe + Mg) ranging from 0.25–0.91 were analyzed by Mössbauer spectroscopy. The spectra were computer fitted to Lorentzian line shapes and consisted of two doublets arising from Fe^{2+} in the two non-equivalent octahedral sites *M*1 and *M*2 and two doublets due to Fe^{3+}. Nuclear quadrupole splitting of ^{57}Fe in biotite is strongly dependent on temperature, indicating iron is in the high spin configuration. Isomer shifts indicate that the iron-oxygen bonds are predominantly of ionic character but with a larger covalent participation compared to the Fe–Mg-chain silicates.

Iron distribution between *M*1 and *M*2 sites is generally found quite disordered.

Introduction

Biotite is an important rock-forming mineral which occurs in a variety of geological environments. It forms throughout a wide range of metamorphic *PT*-conditions and is also an abundant constituent of acid igneous rocks. The widespread occurrence of biotite correlates with the extensive compositional variation of biotites which have formed under different conditions. However, the complex solid solutions observed in trioctahedral micas cause the composition of biotite to meet not only the temperature and pressure conditions which prevail during the formation of the mineral but also the activities and partial pressures of Al, H_2O, H_2, and O_2, *etc.* The stability of micas at different conditions is discussed by Ramberg (1952), Kretz (1959), Saxena (1966, 1968), and Annersten (1968). These studies are based on the intercrystal distribution of elements between micas and other coexisting minerals. Biotite stability was also investigated experimentally by Wones and Eugster (1965), who related the Fe/Mg-ratio of biotite to temperature-pressure, water fugacity, and the partial pressure of oxygen.

Major interest is also directed towards relation of the Fe-Mg distribution between coexisting iron- magnesian silicates with the intracrystalline distribution (Mueller, 1962; Grover and Orville, 1969). Such intracrystalline distribution studies have been facilitated by the introduction of Mössbauer spectroscopy, which proved useful in silicate mineralogy (Bancroft, Maddock, and Burns, 1967). Refined Mössbauer studies of the distribution of iron within pyroxenes were presented by Bancroft, Burns, and Howie (1967), Evans, Ghose, and Hafner (1967), and Virgo and Hafner (1970). Amphiboles have been investigated by Bancroft and Maddock (1967) and Hafner and Ghose (1971). Mössbauer studies of micas, which have been presented by Pollak, de Coster, and Amelinckx (1962) Bowen, Weed, and Stevens (1969), Häggström, Wäppling, and Annersten (1969a,b) and Annersten *et al* (1971) were all of a more or less exploratory nature. However, investigations by Hogg and Meads (1970) and Hogarth, Brown, and Pritchard (1970) showed that considerable variations exist in the Mössbauer parameters of micas. Nevertheless, no specific effort was made to correlate these results with the crystal-chemical features and conditions of formation of the micas.

The present investigation concerns biotite samples representing different compositions and formation conditions, and care is taken to correlate the observed Mössbauer parameters with the physical-chemical parameters of the micas.

Crystal Chemical Features of Trioctahedral Micas

No accurate structure determinations of natural biotites have been undertaken. The basic structural feature of micas, however, is a composite sheet in which octahedrally coordinated cations (Fe^{2+}, Fe^{3+}, Mg and minor Al, Ti, and Mn) are sandwiched be-

[1] Present address: Department of Geosciences, Philipps-Universität, D-3550 Marburg/Lahn, West Germany.

tween two identical layers of Si–Al–O_4-tetrahedrons, the apical oxygens pointing towards the octahedral layer. Each of the cations in the octahedral sites is coordinated with four oxygen and two hydroxyl ions (or occasionally F^-). The principal mica polymorphs (1*M*, 2*M*, and 3*T*) reported by Hendricks and Jefferson (1939) and Smith and Yoder (1956) differ only in the stacking sequence of the layers, which does not influence the octahedral site symmetry. This is the reason why no attempt has been made in these studies to determine the polymorphic state.

More recent refinements of the structure of the trioctahedral micas have been given by Wyckoff (1953), Donnay *et al* (1964), and Franzini and Schiafino (1964). The octahedral sites can be considered to be distorted octahedrons which can be subdivided into two types on the basis of site symmetry (Fig. 1). One of the site types *M*1, which has apical hydroxyl ions, has the symmetry $2/m$ whereas the other position *M*2, where the hydroxyl ions occupy one shared edge of the octahedron, has the symmetry 2. In the mica unit cell there are twice as many *M*2 sites as *M*1 sites. For synthetic ferri-annite Donnay *et al* (1964) reported the average bond length around Fe^{2+} in *M*1 to be 2.106 Å and around Fe^{2+} in *M*2, 2.107 Å. From Mössbauer studies Häggström *et al* (1969b) suggested that the *M*1 site is slightly more distorted than the *M*2 site and that the site symmetry of both *M*1 and *M*2 is probably

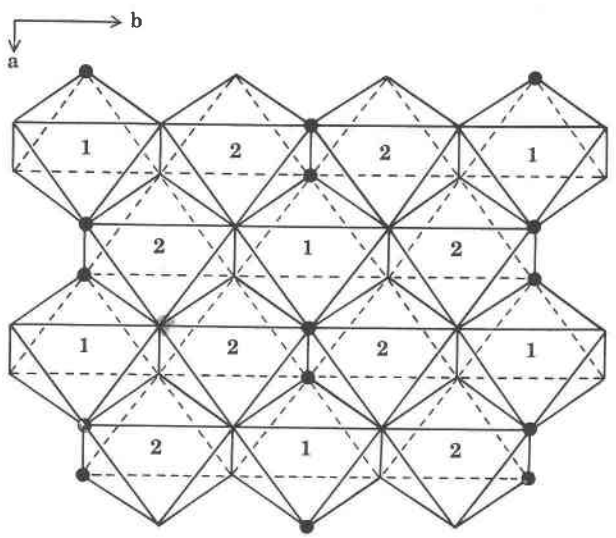

● = OH – ion

FIG. 1. Schematic view of the octahedral layer in trioctahedral mica showing the ideal coordination of cations in *M*1 (1) and *M*2 (2) positions.

triclinic. The iron-ligand distances in the biotite structure, which are comparable to those found in amphiboles and pyroxenes wherein iron occurs in its high-spin configuration (Bancroft, Burns, and Howie, 1967), suggest that it is reasonable to assume high-spin iron also in biotite.

Franzini and Schiafino (1964) suggested the possibility that substitution of Fe^{2+} and Fe^{3+} for Mg produces a small contraction of the octahedral layer although the reported values were all within the limit of error. Donnay *et al* (1964) also reported very similar values of the Mg–O and Fe–O bond lengths in ferri-phlogopite and ferri-annite; the distances are 2.115 Å ± 0.011 and 2.123 Å ± 0.011 respectively. This may also be evident from the fact that the reported values of the quadrupole splittings of Fe^{2+} in micas are constant in spite of large differences in the Mg/Fe-ratio (Häggström *et al*, 1969a,b). It may therefore be concluded that no large change in site symmetry will take place due to the Fe-Mg substitution.

The six biotites selected for investigation represent samples of different composition and genesis. Their chemical compositions were determined by microprobe analysis applying the method and corrections described by Dahl (1969). Ferrous-ferric iron ratios were determined by wet-chemical methods except for sample 6, where too little material was available.

From Table 1 it is seen that more than 80 percent of the octahedral sites are populated by iron and magnesium and that the rest are filled by Ti, Al, Mn, or left vacant. In most biotites octahedral occupancy is significantly less than the available number of octahedral sites in the mica unit cell. In trioctahedral micas there is generally a decrease in octahedral occupancy with increase in octahedral trivalent cation contents. This can also be recognized in the presently studied samples except for sample 6. That sample has a significant Si–Al-deficiency in the tetrahedral sites which makes it possible to consider Fe^{3+} or Ti in tetrahedral coordination (Saxena, 1966). This problem may be tackled by Mössbauer spectroscopy and will be further discussed below.

The vacant sites in dioctahedral micas are the *M*1 positions; however, this is not necessarily the case in trioctahedral micas. Moreover, the solid solution between di- and trioctahedral micas is very restricted. Preferred occurrence of vacancies in one of the two non-equivalent site types in the structure may, however, be achieved by the clustering of the vacancies around the ions of highest valence, such as Fe^{3+}, Al,

or Ti according to the Pauling local neutrality principle. Also the stronger polarization power of Fe^{2+}, Fe^{3+}, Al, and Ti as compared to Mg will probably induce these ions to enter octahedrons adjacent to vacant positions. It therefore seems important to consider the vacancies when discussing the distribution of elements within the mica structure.

Mössbauer Experiments

Mössbauer experiments were performed using a 400 channel analyzer operating in time mode in conjugation with a constant acceleration electromechanical velocity generator. The velocity wave had a symmetrical "saw-tooth" shape. The velocity increment per channel for all biotite spectra was 0.0402 mm/sec. Due to the symmetrical velocity shape, two mirror symmetric spectra (200 channels) were obtained simultaneously. In each case left and right side spectra were analyzed separately, and the data in Table 2 are average values. The number of counts per channel varied between $3 \cdot 10^6$ and $8 \cdot 10^6$ per spectrum.

The routine experiments were made with the absorber at room temperature, but some experiments were performed with the absorber at liquid nitrogen temperature or at elevated temperature (Fig. 1). The source, Co^{57} in Pd foil, was always kept at room temperature and the 14.4 keV-rays were detected with a Xe and CO_2 filled proportional counter. The distance between the source and absorber was kept constant at 10 cm in all experiments. Absorbers were made by mixing 30–40 mg powdered biotite with 100 mg of lucite. The mixture was pressed at 130°C to form thin discs with 1/2 inch diameter. The density of natural iron of the absorbers was thus kept constant at 3.5 mg/cm². The pressing produced a preferred orientation of the mica grains in the absorbers and hence asymmetry of the doublet intensity. This is explained by the fact that preferred orientation produces an ordering of the principal axis, and the ratio of relative transition probabilities of the quadrupole doublet will be dependent on the angle between the axis of symmetry and the incident gamma rays (Wertheim, 1964). Changing the angle also produces a change in the asymmetry ratio between the quadrupole lines as reported by Häggström *et al* (1969a).

Absorbers producing no preferred orientation were made by applying heat without pressure on the mixture and allowing the mixture to sinter at 130°C.

All spectra were analyzed with the aid of a computer program (Agresti, Bent, and Persson, 1969) which performs a least squares fit of the absorption doublets under the assumption of their Lorentzian shape. Because of the close overlap of the absorption lines and the difficulty in obtaining the quantitative iron distribution in the structure, the fitting procedure of the spectra will be discussed in some detail.

The program fits the physical parameter, nuclear moments, and hyperfine fields to the experimental data. In the fit the line widths of all component peaks were kept equal, which is justified because the absorber can be considered to be thin, and relaxation effects are of no importance in micas. Moreover, studies of several silicate minerals have indicated very uniform half-widths (Bancroft and

TABLE 1. Microprobe Analysis of Biotites

Sample	1	2	3	4	5	6
SiO_2	35.9	35.6	34.3	35.6	41.2	30.8
Al_2O_3	15.2	16.7	14.2	13.1	12.2	11.8
TiO_2	3.5	2.0	3.4	5.8	1.2	5.2
Fe_2O_3 +)	5.6	8.0	8.4	5.0	2.7	nd
FeO	13.8	13.5	23.6	16.7	9.3	38.4 ++)
MgO	11.1	10.2	1.9	10.0	20.1	2.1
MnO	0.13	0.12	0.38	0.08	0.11	0.18
Na_2O	nd	0.1	0.1	0.0	0.2	nd
K_2O	9.7	9.0	9.3	9.7	9.8	7.5
Number of ions on basis of 22 oxygens						
Si	5.25	5.39	5.50	5.45	5.92	5.20
Al^{IV}	2.75	2.61	2.50	2.35	2.05	2.33
Al^{VI}	0.33	0.36	0.18	-	-	-
Ti	0.37	0.23	0.40	0.67	0.12	0.65
Fe^{3+}	0.60	0.91	1.00	0.56	0.29	-
Fe^{2+}	1.66	1.70	3.16	2.13	1.11	5.42
Mg	2.39	2.30	0.46	2.27	4.30	0.52
Mn	0.015	0.015	0.05	0.010	0.050	0.025
Na	-	0,03	0.03	0.01	0.05	-
K	1.78	1.73	1.89	1.89	1.79	1.60
Fe/Fe + Mg	0.42	0.53	0.90	0.51	0.25	0.91

+) wet chemical determination

++) total iron as FeO

1. *GGU sample 60508. Biotite from high amphibolite facies gneiss SW Greenland.*
2. *GGU sample 84332. Biotite from low amphibolite facies gneiss SW Greenland.*
3. *Biotite from Revsund Granite, Sweden. Gorbatschev (1969).*
4. *Biotite from charnokite, Varberg, Sweden. O. Dahl (unpublished).*
5. *Biotite from metamorphosed iron formation, Sweden. Annersten* et al *(1971).*
6. *Biotite from titano-ferrous meta diabase, Nordingrå, Sweden. A. Lindh (unpublished).*

TABLE 2. Mössbauer Parameters for Iron in Biotites (mm/sec)

Sample	L.W.	Fe^{2+} M1 I.S.	Fe^{2+} M1 ΔE_Q	Fe^{2+} M2 I.S.	Fe^{2+} M2 ΔE_Q	Fe^{3+} M1 I.S.	Fe^{3+} M1 ΔE_Q	Fe^{3+} M2 I.S.	Fe^{3+} M2 ΔE_Q	χ^2
1[a]	.34	1.03	2.10	1.06	2.56	0.41	1.02	0.43	0.50	3.4
1[b]	.31	1.18	2.51	1.19	2.85	0.40	1.20	0.42	0.62	3.8
1[c]	.29		0.63	1.11			0.22	0.57		2.4
2[a]	.31	1.05	2.19	1.07	2.62	0.50	0.72	0.52	0.57	4.3
3[a]	.32	1.01	2.20	1.06	2.60	0.43	0.93	0.40	0.50	4.6
4[a]	.34	1.02	2.13	1.06	2.56	0.41	0.74	0.39	0.57	3.7
5[a]	.34	1.03	2.21	1.05	2.58	0.51	1.17	0.46	0.65	5.7
6[a]	.33	1.05	2.12	1.05	2.57	0.50	0.88	0.54	0.34	3.9

a) absorber at room temperature
b) absorber at liquid nitrogen temperature
c) absorber at 132° C

Isomer shifts are given relative to metallic iron. Relative standard deviation for the line widths (L.W.) are ± 1%. The errors for Fe^{2+} I.S. and ΔE_Q are within ± 0.01 and 0.02 mm/s respectively. Errors for Fe^{3+} I.S. and ΔE_Q are within ± 0.02 and 0.04 mm/s respectively.

Williams, 1969; Burns and Greaves, 1971). Saturation effects can be neglected because the absorber density is small.

The preferred orientation of the mica grains affects the Mössbauer spectra by producing asymmetric intensities of the iron doublets. Assuming that all sites have axial symmetry around the same axis, the intensity ratio can be constrained to be the same for all ferrous doublets, but *reciprocal* of the ferric iron doublets, because the electric field gradient has opposite signs in the two types of iron ions (Ingalls, 1964). Actually the local symmetry around the iron nucleus is lower than axial, and all intensity ratios should be different. Spectra taken at different 'grade of randomization' indicate, however, that the deviation from axial symmetry is small when preferred orientation is small (as in the present case) and that the area ratio is not changed significantly.

The goodness of fit is given by the Q^2-value, which is the statistically weighted sum over all data points of the squares of the differences between the experimental data and the postulated theoretical function (F) fitted to the experimental data. Q^2 has the explicit form

$$Q^2 = \sum_{k=1}^{200} \frac{1}{Y_k} (F(x_k; \alpha_1, \cdot\alpha_j, \cdot\alpha_p) - Y_k)^2$$

where $F(x_k, \alpha)$ is the value of the theoretical function evaluated at the k^{th} data point and Y_k is the number of counts in the same channel. The function is determined by the p variable parameters α_j, the present experimental spectrum consisting of 200 points, each with a velocity denoted x_k. The final smallest value of Q^2 is normalized by dividing by the number of degrees of freedom to give the chi square (χ^2) fit. Typical fits for the present spectra (17 free variables) have χ^2 values between 2.4–5.7 (see Table 2) depending on the number of counts per channel (see above).

Results

Typical Mössbauer spectra of biotites are shown in Figure 2. The experimental data are shown by points and the full line drawn through the points is the summarized computer-fitted spectra. Thin lines show the position of the individual doublets. The main features of the spectra are (1) two intense peaks at around 0 and 2.2 mm/sec which indicate isomer shifts and quadrupole splittings characteristic of high-spin ferrous iron in octahedral coordination, and (2) one weak line at 0.5 mm/sec referred to ferric iron. There are clearly two Fe^{2+} lines in the high velocity region (Häggström *et al*, 1969b) and fitting two ferrous iron doublets also significantly reduces χ^2 in comparison with the assumption of only one doublet. Assuming only one ferric iron doublet resulted in broad (0.6–0.7 mm/sec) ferric iron absorption lines which indicated that ferric iron populates more than one type of site. Some of the spectra also indicate serious deviation from Lorentzian line shape of the ferric iron peak. Two ferric iron doublets were fitted to the spectra.

In the first stage of the computer fitting for the two ferric iron doublets, isomer shifts were constrained to be the same for both the doublets. This resulted in large chi square values (6–9) but, after releasing the isomer shift constraint, the chi square values decreased to around 3–4. At the same time, however, the isomer shift values diverged for the two ferric iron doublets. The difference in shifts is, however, small and, considering the close overlap, the isomer shifts are the same within the experimental error. The reported shifts (Table 2) are also in good agreement with ferric iron shifts reported for other Fe–Mg silicates with similar structure (Bancroft, and Williams, 1969, Burns and Greaves, 1971).

All spectra thus gave the best fit assuming two ferrous iron doublets and two ferric iron doublets, which is also in accordance with the proposed crystal structure. The hyperfine parameters deduced from the spectra of biotites are given in Table 2.

The assignment of the ferrous iron peaks to the different structural sites is made in accordance to the

discussion in Häggström *et al* (1969b). It indicates that the more intense ferrous iron doublet with the large quadrupole splitting belongs to iron in *M*2 sites and that the ferrous iron showing the smaller splitting is due to iron in *M*1 sites.

Site assignment of ferric iron is less evident. Ferric iron, however, has spherical electron configuration, and a contribution to the quadrupole splitting will only arise from the electric field gradient from the structure. As shown by Ingalls (1964) the contribution from the structure for ferrous iron is opposite to the dominating electronic contribution, which results in a decreasing quadrupole splitting for ferric iron. Octahedral ferric iron with the largest observed quadrupole splitting will thus be assigned to the octahedral site whereas ferrous iron shows the smallest splitting, which is the *M*1 site.

Table 2 reveals some fluctuation of the hyperfine parameters, especially for ferric iron. This may partly represent bad resolution or the contribution by compositional effects, vacancies, and octahedral aluminum to these parameters. Tetrahedral ferric iron in micas is characterized by having small isomer shifts around 0.15 mm/sec relative to metallic iron (Hogarth *et al,* 1970; Annersten *et al,* 1971). No Mössbauer spectroscopic evidence is found for ferric iron in tetrahedral coordination in the present samples although chemical analysis may indicate the possibility of ferric iron in this position in sample 6. It may therefore be concluded that the major part of the ferric iron in this sample is octahedrally coordinated, which leaves the possibility of Ti being the ion which together with Si and Al enters the tetrahedral sites in sample 6.

Iron site occupancy (Table 3) has been calculated on the assumption that the recoilless fraction for iron is identical in the two non-equivalent sites and independent of composition. Spectra of synthetic annite were taken to clarify this, but the presence of ferric iron in these samples gave rise to complications. Site populations obtained from liquid nitrogen spectra disagree to some extent with those recorded at room temperature for the same sample, which may indicate a temperature dependency of the iron site population and hence a difference in the Debye temperature for iron in *M*1 and *M*2. Since the recoil-free fraction for different sites tends toward a uniform value at low temperature, spectra recorded at liquid nitrogen temperature may yield more accurate values on iron site occupancy than those taken at room temperature. The closer overlap of the ferrous iron doublets found at 77 K (see Fig. 2) will, however, further decrease the resolution and may also reflect the difference in the obtained site population.

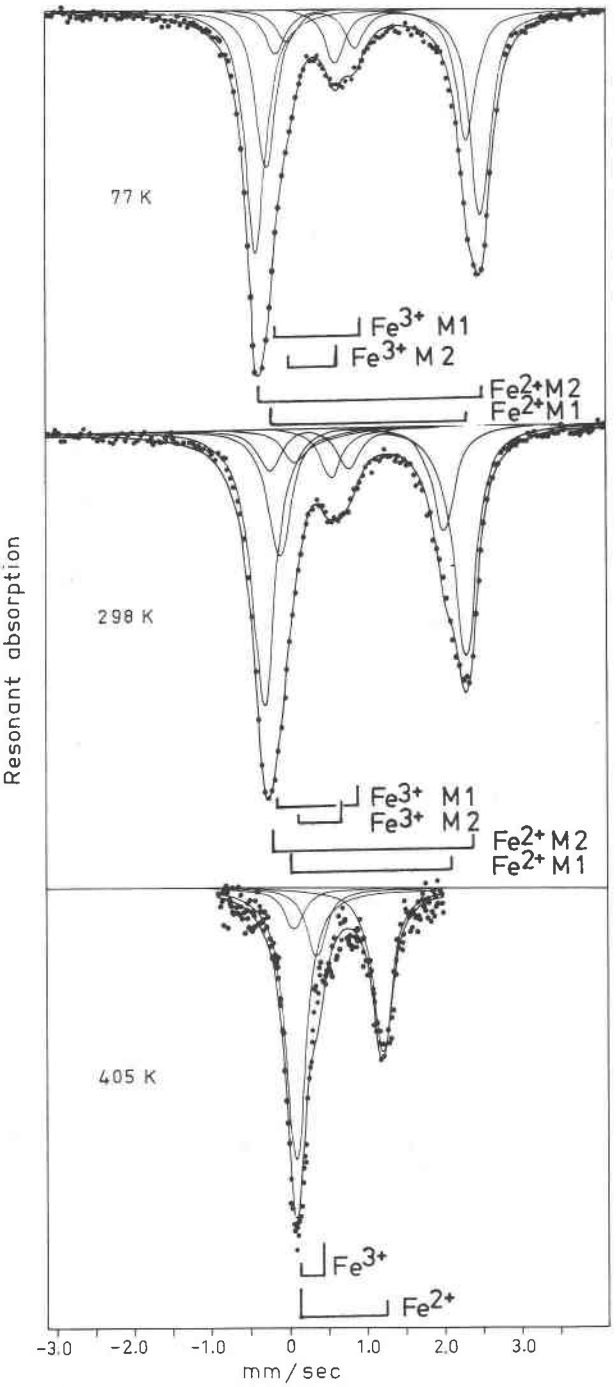

FIG. 2. Mössbauer spectra of biotite (sample 1) at different temperatures. The pronounced asymmetry in the high temperature spectrum is due to the preferred orientation of the mica grains on a thin beryllium disc.

TABLE 3. Iron Distribution in Mica Obtained from Mössbauer Spectra

Sample	Fe^{2+} M1	Fe^{2+} M2	Fe^{3+} M1	Fe^{3+} M2
1[a]	0.30	0.31	0.07	0.07
1[b]	0.35	0.28	0.09	0.06
2[a]	0.25	0.41	0.16	0.03
3[a]	0.44	0.61	0.16	0.13
4[a]	0.44	0.33	0.07	0.07
5[a]	0.16	0.21	0.06	0.03
6[a]	0.61	0.79	0.25	0.13

a) room temperature spectra
b) liquid nitrogen spectra

There is so far no evidence that the recoil-free fractions are significantly different at non-equivalent octahedral sites with similar types of surrounding ligands in ferro-magnesian silicates (Burnham *et al,* 1971).

A spectrum of exploratory nature was measured at 132°C for only a few hours in order not to destroy the hydrous mica (Fig. 2). This shows a still closer overlap and a decrease in the quadrupole splitting so that only two doublets are resolved.

Room temperature therefore seems to be the most suitable temperature at which Mössbauer spectra of biotites should be recorded in spite of the still inconvenient overlap.

Crystal Chemical Interpretation and Discussions

Isomer shifts

The dependence of the isomer shifts on the chemical composition (Fe/Mg ratio) is very slight in biotites, a feature also found for other Fe, Mg silicates.

Since the isomer shift measures the charge density around the nucleus, some qualitative conclusions on the state of bonding of iron at the octahedral sites in biotites can be made from the observed shifts and compared to other Fe, Mg silicates. This comparison is best made on shifts determined at low temperature in order to minimize the contribution from the thermal shift to the total measured shift (isomer shift). The magnitude of the isomer shifts (Table 4) for the selected silicate sites may be interpreted as a measure of the covalent participation in a predominantly ionic bonding character of the Fe–O bonds. The noticeable decrease in the isomer shifts in going from orthopyroxene to biotite (Table 4) indicates increased electron delocalization at the iron nucleus in the respective sites. This suggests an increased covalent bonding character of iron at the octahedral sites of the selected silicate series.

There seems to be little evidence that the stereochemical difference (Table 4) between the sites may result in so large changes in isomer shifts (Hafner and Ghose, 1971). Interestingly, the isomer shifts correlate with increasing degree of polymerization in the above silicate series. With increasing polymerization, the effective polarization power of Si increases at the unshared oxygen (Ramberg, 1954). This results in a lower orbital overlap potential with a coordinated Fe ion in octahedral site. However, increased substitution of Al for Si, which often accompanies increased polymerization in silicates (see Table 4), will counteract the increasing polarization because of the smaller polarization power of Al. Thus increased Al substitution in tetrahedral sites will result in an increased orbital overlap between the oxygen-iron bonds and hence a more covalent character of the bonds in micas. More detailed studies on this phenomena may be performed on actinolites with variable $Si–Al^{IV}$ ratio. In addition we may also expect presence of OH and F in amphiboles and micas to influence bonding character.

Quadrupole splitting

The strong temperature dependence of the quadrupole splittings of the two major doublets clearly shows these lines to arise from high spin ferrous iron.

The major structural-chemical factors contributing to the quadrupole splitting in silicates are, according to Bancroft, Maddock, and Burns (1967), (1) dis-

TABLE 4. Isomer Shifts and Crystal Chemical Data for Fe^{2+} in Octahedral Coordination in Some Fe–Mg silicates

Silicate	Average Fe-O distance A	Shortest Fe-O distance A	Isomer shift[a] 77 K	$Al^{IV}/Al^{IV}+Si$
ORTHOPYROXENE M1	2.123[b]	2.076[b]	1.29[b]	0.004[b]
CUMMINGTONITE M1M2M3	2.103[c]	2.070[c]	1.27[c]	0.009[d]
ACTINOLITE M1	2.107[e]	2.090[e]	1.23[f]	0.04[f]
BIOTITE M1	2.106[g]	2.070[g]	1.18	0.34

a) relative to metallic iron
b) Burnham et al (1971)
c) Hafner et al (1971)
d) Mueller (1960)
e) Mitchell et al (1971)
f) Burns et al (1971)
g) Donnay et al (1964)

tortion of the octahedral polyhedra from cubic symmetry and (2) the field gradient due to neighboring cations in biotites such as Mg, Fe^{2+}, Fe^{3+}, Ti, Al, or vacancies.

According to Ingalls (1964), the differences in quadrupole splitting of Fe^{2+} show the *M*1 site to be more distorted than the *M*2 site. Thus ferrous iron splittings are similar for *M*2 sites but show some variation for *M*1. In view of the results reported by Donnay *et al* (1964), any drastic changes in the distortion of the *M*1 and *M*2 polyhedrons in micas due to substitutions of cations are unlikely. Changes in the quadrupole splittings for a given site are thus more likely to arise from the change of field gradients due to difference in adjacent octahedral cation occupancy. This effect is also expected to be larger for the *M*1 sites because of the relatively stronger influence on this site from six adjacent *M*2 sites, as compared to only three neighboring *M*1 sites (and three *M*2 sites) around *M*2 sites.

One of the largest ferrous iron splittings in *M*1 is shown by sample 5, which is also the sample richest in Mg. Similar features have been found in cummingtonite and pyroxene by Bancroft, Maddock, and Burns (1967). Comparatively large splittings in *M*1 are, however, also found in the iron-rich samples 2 and 3, which suggests that factors other than the Fe/Mg ratio contribute to the field gradient. These may reflect changes in the effective charges from the shared oxygen ligands as caused by presence of vacant sites or variations in charges of the cations neighboring these oxygen ligands, but this is difficult to calculate quantitatively at present.

Distribution of Iron Between Non Equivalent Sites in Biotites

Iron site occupancy calculated from the observed spectra and known chemical compositions is shown in Table 3 and plotted in Figure 3. The figures are obtained from a mica unit cell containing four *M*2 and two *M*1 positions. The site occupancy for Fe^{2+} is believed to be correct within ± 10 percent.

From Figure 3 it is seen that ferrous iron is slightly enriched in the *M*2 positions except in samples 1 and 4, which show a more disordered distribution. Generally a marked partitioning of Fe^{2+} into one specific type of octahedral site in ferro-magnesian silicates is a consequence of highly distorted oxygen polyhedrons favouring Fe^{2+} (Ghose, 1961; 1964). In mica, however, *M*2 is the more symmetric site, and no obvious reason for this ordering is found.

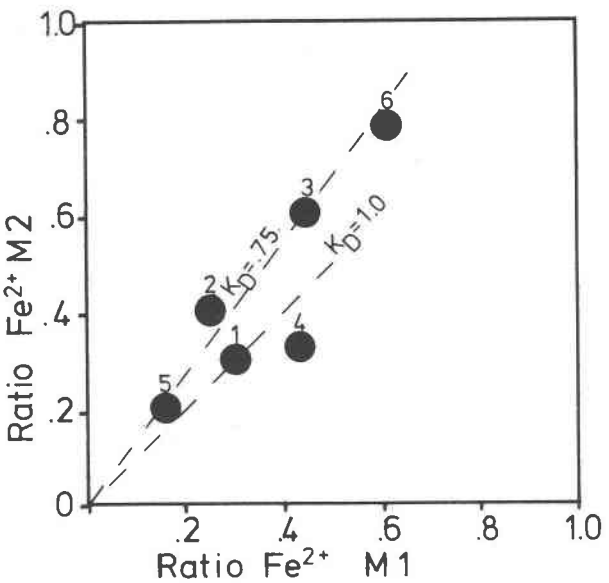

FIG. 3. Ferrous iron distribution in biotite samples obtained from Mössbauer spectra.

The deviating samples 1 and 4 (Fig. 3) represent biotites from high-grade metamorphic rocks. Ghose and Hafner (1967) and Virgo and Hafner (1969) found an increased Fe/Mg disorder in orthopyroxenes from volcanic rocks and in heated orthopyroxenes respectively. Similar features are reported by Schürmann and Hafner (1971) for heated cummingtonite. These minerals can be described as simple binary solid solutions and are also found to exhibit rapid disordering at increasing temperatures. Biotite, however, can be considered as a complex solid solution with a short-range order associated with high, compositionally dependent, exchange energies. Accordingly, in biotites, composition rather than temperature may be the determining factor of the intracrystalline element distribution. More data are needed to clarify the solid solution in micas.

Ferric iron

A detailed discussion of ferric iron in biotite is difficult in view of the larger errors reported for the ferric iron parameters.

An estimation of the accuracy of the intensity for the ferric iron may, however, be made from comparison with wet chemical analysis of the Fe^{3+} content in biotites (see Table 5). Although there is a very general agreement between the two methods (except sample 2), wet chemical methods always seem to overestimate the ferric iron content. This is not unexpected since the analytical technique is

TABLE 5. Ratio Fe^{3+}/Total Iron

Sample	1	2	3	4	5
chemical analysis	0.26	0.34	0.24	0.20	0.20
Mössbauer spectra	0.17	0.13	0.20	0.17	0.18

known for its difficulties in preventing ferrous iron from oxidation when bringing silicates into solution, especially with titanium (Ti^{3+} ?) present in biotite. It is therefore believed that Mössbauer spectroscopy provides a more accurate method for estimating the ferric iron content in biotites.

Acknowledgments

I am much obliged to Professor Stefan S. Hafner for putting his Mössbauer equipment at my disposal during my short stay at the Department of Geophysical Sciences, University of Chicago. For valuable discussions and critical reading of the manuscript I thank Professor Hans Ramberg, Dr. R. Gorbatschev, Dr. B. Lindqvist, and Dr. L. Häggström. For donating samples used in this investigation I thank Dr. O. Dahl and Dr. A. Lindh.

Financial support was provided by grants from the U.S. National Science Foundation GA14811A (S. Hafner) and the Natural Science Research Council of Sweden.

References

AGRESTI, D., M. BENT, AND B. PERSSON (1969) A versatile computer program for analysis of Mössbauer spectra. *Nucl. Instr. Meth.* **72,** 235–236.

ANNERSTEN, H. (1968) A mineral chemical study of a metamorphosed iron formation in northern Sweden. *Lithos,* **1,** 374–397.

———, AND T. EKSTRÖM (1971) Distribution of major and minor elements in coexisting minerals from a metamorphosed iron formation. *Lithos,* **4,** 185–204.

———, S. DEVANARAYANAN, L. HÄGGSTRÖM, AND R. WÄPPLING (1971) Mössbauer study of synthetic ferriphlogopite $KMg_3Fe^{3+}Si_3O_{10}(OH)_2$. *Phys. Stat. Sol.* **48b,** 137–138.

BANCROFT, G. M., A. G. MADDOCK, AND R. G. BURNS (1967) Application of the Mössbauer effect to silicate mineralogy. *Geochim. Cosmochim. Acta,* **31,** 2219–2246.

———, R. G. BURNS, AND R. A. HOWIE (1967) Determination of the cation distribution in the orthopyroxene series by the Mössbauer effect. *Nature,* **213,** 1221–1223.

———, AND A. G. MADDOCK (1967) Determination of the cation distribution in the cummingtonite-grünerite series by the Mössbauer effect. *Am. Mineral.* **52,** 1009–1026.

———, AND P. G. L. WILLIAMS (1969) Mössbauer spectra of omphacites. *Mineral. Soc. Am. Spec. Pap.* **2,** 59–65.

BOWEN, L. H., S. B. WEED, AND R. G. STEVENS (1969) Mössbauer study of micas and their potassium-depleted products. *Am. Mineral.* **54,** 72–84.

BURNHAM, C. W., Y. OHASHI, S. S. HAFNER, AND D. VIRGO (1971) Cation distribution and atomic thermal vibrations in an iron-rich orthopyroxene. *Am. Mineral.* **56,** 850–876.

BURNS, R. G., AND C. J. GREAVES (1971) Correlations of infrared and Mössbauer site population measurements of actinolites. *Am. Mineral.* **56,** 2010–2033.

DAHL, M. (1969) Standard and correction methods used in electron microprobe analysis of biotites, amphiboles, pyroxenes, and plagioclases. *Neues Jahrb. Mineral. Abhandl.* **110,** 210–225.

DONNAY, G., N. MORIMOTO, H. TAKEDA, AND J. D. H. DONNAY (1964) Trioctahedral one-layer micas. I. Crystal structure of synthetic iron mica. *Acta. Crystallogr.* **17,** 1369–1373.

EVANS, B. J., S. GHOSE, AND S. S. HAFNER (1967) Hyperfine splitting of ^{57}Fe and Fe-Mg order disorder in orthopyroxenes. *J. Geol.* **75,** 306–322.

FRANZINI, M., AND L. SCHIAFFINO (1964) On the crystal structure of biotites. *Z. Kristallogr.* **119,** 297–309.

GHOSE, S. (1961) The crystal structure of cummingtonite. *Acta Crystallogr.* **14,** 622–627.

——— (1964) Mg^{2+} — Fe^{2+} order in orthopyroxene $Mg_{0.93}Fe_{1.07}Si_2O_6$. *Z. Kristallogr.* **122,** 82–99.

———, AND S. S. HAFNER (1967) Mg^{2+}–Fe^{2+} distribution in metamorphic and volcanic orthopyroxenes. *Z. Kristallogr.* **125,** 157–162.

GORBATSCHEV, R. (1969) Element distribution between biotite and Ca-amphibole in some igneous or pseudo-igneous plutonic rocks. *Neues Jahrb. Mineral. Abhandl.* **111,** 314–342.

GROVER, J. E., AND P. M. ORVILLE (1969) The partitioning of cations between coexisting single- and multi-site phases with application to the assemblages orthopyroxene-clinopyroxene and orthopyroxene-olivine. *Geochim, Cosmochim. Acta,* 205–226.

HAFNER, S. S., AND S. GHOSE (1971) Iron and magnesium distribution in cummingtonites $(FeMg)_7Si_8O_{22}(OH)_2$. *Z. Kristallogr.* **133,** 301–326.

HÄGGSTRÖM, L., R. WÄPPLING, AND H. ANNERSTEN (1969a) Mössbauer study of oxidized iron silicate minerals. *Phys. Stat. Sol.* **33,** 741–748.

———, ———, AND ——— (1969b) Mössbauer study of iron-rich biotites. *Chem. Phys. Lett.* **4,** 107–108.

HENDRICKS, S. B., AND M. JEFFERSON (1939) Polymorphism of the micas with optical measurements. *Am. Mineral.* **24,** 729–738.

HOGARTH, D. D., F. F. BROWN, AND A. M. PRITCHARD (1970) Biabsorption, Mössbauer spectra and chemical investigation of five phlogopite samples from Quebec. *Can. Mineral.* **10,** 710–722.

HOGG, C. S., AND R. E. MEADS (1970) The Mössbauer spectra of several micas and related minerals. *Mineral. Mag.* **37,** 606–614.

INGALLS, R. (1964) Electric-field gradient tensor in ferrous compounds. *Phys. Rev.* **133,** A787–795.

KRETZ, R. (1959) Chemical study of garnet, biotite and hornblende from gneisses of southwestern Quebec, with special emphasis on the distribution of elements in coexisting minerals. *J. Geol.* **67,** 371–402.

MUELLER, R. F. (1960) Composition characteristics and equilibrium relations in mineral assemblages of a metamorphosed iron formation. *Am. J. Sci.* **258,** 449–497.

——— (1962) Energetics of certain silicate solid solutions. *Geochim. Cosmochim. Acta,* **26,** 581–598.

POLLAK, H., M. DE COSTER, AND S. AMELINCKX (1962) Mössbauer effect in biotite. *Phys. Stat. Sol.* **2,** 1652–1656.

RAMBERG, H. (1952) *The Origin of Metamorphic and Metasomatic Rocks.* Univ. Chicago Press, Chicago, Illinois.

——— (1954) Relative stabilities of some simple silicates as related to the polarization of the oxygen ions. *Am. Mineral.* **39,** 256–271.

SAXENA, S. K. (1966) Distribution of elements between coexisting muscovite and biotite and crystal chemical role of titanium in micas. *Neues Jahrb. Mineral. Abhandl.* **105,** 1–17.

——— (1968) Chemical study of phase equilibria in charnocites, Varberg, Sweden. *Am. Mineral.* **53,** 1674–1695.

SCHÜRMANN, K., AND S. S. HAFNER (1971) Temperature dependent distribution of magnesium and iron in cummingtonites. *Nature,* **231,** 155–156.

SMITH, J. V., AND H. S. YODER (1956) Experimental and theoretical studies of the mica polymorphs. *Mineral. Mag.* **31,** 209–235.

WERTHEIM G. K. (1964) *Mössbauer Effect. Principles and Applications.* Academic Press, N.Y.

VIRGO, D., AND S. S. HAFNER (1969) Fe^{2+}–Mg order-disorder in heated pyroxenes. *Mineral. Soc. Am. Spec. Pap.* **2,** 67–81.

———, ——— (1970) Fe^{2+}–Mg order-disorder in natural orthopyroxenes. *Am. Mineral.* **55,** 201–233.

WONES, D. R., AND H. P. EUGSTER (1965) Stability of biotite. Experiment, theory, and application. *Am. Mineral.* **50,** 1228–1272.

WYCKOFF, R. G. W. (1953) *Crystal Structures, Vol. III.* Interscience Pub., New York.

Manuscript received, December 4, 1972; accepted for publication, September 10, 1973.

American Mineralogist, Volume 59, pages 152–158, 1974

Development of Long Basal Spacings in Chlorites by Thermal Treatment

G. W. BRINDLEY, AND TIEN-SHOW CHANG

Geosciences Department, Pennsylvania State University, University Park, Pennsylvania

Abstract

Alterations of micas, vermiculite, and smectites, mainly montmorillonite, have provided numerous examples of the development of long spacings, but such spacings have not been developed previously from chlorites by laboratory processes. Magnesian chlorites, both natural and synthetic materials, are shown to develop long spacings of about 27 Å when the hydroxide interlayers are decomposed (dehydroxylated). A model is developed with a regular alternating sequence of A- and B-type interlayers, and with small displacements of the talc-like layers which gives calculated X-ray (00*l*) intensities in general agreement with the observed peak intensities. Broadened odd-order reflections from the long spacing are thought to indicate "mistakes" in the modified layer sequence, while the even orders, corresponding to the usual 14 Å spacing, show sharp reflections.

Introduction

Numerous examples are known of layer silicates having basal spacings greater than 20 Å. These long spacings are produced by regular successions of layers of two kinds, generally in a 1:1 ratio. Typical examples are rectorite (allevardite), corrensite, tosudite, and tarasovite. The component layers are usually similar to those in micas, smectites, vermiculite, chlorite; *i.e.,* they are 2:1 type layers with various interlayer arrangements. Many laboratory experiments have been made to develop similar long-spacing structures from micas, smectites, and vermiculites, but to the writers' knowledge no chlorites, although they are also 2:1 type layer silicates, have been so modified experimentally until now.

The development of a long-spacing modification of vermiculite was described by Walker (1956) who found during the final stages of dehydration of vermiculite a 20.6 Å phase consisting of an alternating sequence of 11.6 and 9.0 Å components. Evidently the residual water in this structure preferred to occupy every second interlayer rather than to be randomly distributed over all interlayers. Bassett (1959) described the progressive replacement of K^+ ions in biotite by hydrated Mg^{2+} or Ca^{2+} ions to form vermiculite, with hydrobiotite developing as an intermediate phase with alternating K^+ and hydrated R^{2+} interlayers. Sawhney (1967, 1972) obtained similar results when a Ca-vermiculite was exchanged progressively with K^+ or Cs^+ ions; long spacings were developed with Ca^{2+} and K^+ (or Cs^+) ions in alternate layers.

Many authors have discussed the influence of OH dipole orientation on the stability of interlayer cations in mica structures. Bassett (1960), following the earlier work of Tsuboi (1950) and of Serratosa and Bradley (1958a,b), correlated the stabilities of muscovite, biotite, and phlogopite with OH dipole orientations. The increased chemical stability of biotites when oxidized also may be related to a reorientation of the internal OH dipoles (Barshad and Kishk, 1968, 1970; Juo and White, 1969), and the tendency of high-iron biotites to form long-spacing structures when oxidized may involve a similar mechanism (Weed and Leonard, 1968; Farmer and Wilson, 1970). Norrish (1972) has described a mechanism by which changes in one interlayer may influence adjacent interlayers through changes in OH dipole orientation within the 2:1 layers. Thus a considerable body of opinion, supported by many experiments, has developed around the idea that a long-range influence can be transmitted through the 2:1 layer structure by the OH dipoles.

An alternative view, put forward by Sudo, Hayashi, and Shimoda (1962), is that structures containing alternating layers are influenced by a polarity of layer charge distribution in the 2:1 silicate layers. Long basal spacings in micas have been developed